THE JOURNAL OF PHYSICAL CHEMISTRY C
A JOURNAL OF THE AMERICAN CHEMICAL SOCIETY

pubs.acs.org/JPCC

Article

Highly Charged Excitons and Biexcitons in Type-II Core/Crown Colloidal Nanoplatelets

Jordi Llusar and Juan I. Climente*

Cite This: J. Phys. Chem. C 2022, 126, 7152−7157

Read Online

ACCESS | Metrics & More | Article Recommendations | Supporting Information

ABSTRACT: The optoelectronic properties of type-II CdSe/CdTe colloidal nanoplatelets (NPLs) charged with neutral excitons (X^0) have been intensively investigated in the last years. Motivated by the recent experimental progress, here we use effective mass simulations to study the effect of charging core/crown NPLs with a few extra electrons or holes. Emission spectra are calculated for charged excitons (X^n, with $n = 2$ to $n = -3$) and biexcitons (XX). The strong Coulomb interactions within the platelet lead to a number of remarkable properties. For excitons, varying the number of excess charges gives rise to band gap red- and blue-shifts spanning over 100 meV and widely tunable oscillator strength. For biexcitons, the binding energy can be tuned from nearly nonbonding to strongly antibonding (~40 meV) by modulating the core/crown area ratio. We conclude that the number of excess carriers injected into type-II NPLs is a versatile degree of freedom to modulate the optoelectronic properties.

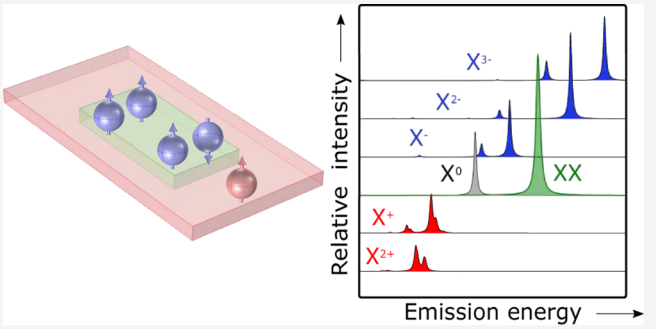

INTRODUCTION

Colloidal nanocrystal heterostructures with a type-II (staggered) band alignment are of interest for the development of optoelectronic applications where controllable spatial separation of electrons and holes is advantageous.[1,2] CdSe/CdTe core−crown nanoplatelets (NPLs) are a prominent example of such structures.[3−5] In these systems, a rectangular CdSe core with a thickness of a few atomic monolayers is laterally surrounded by a CdTe crown. Because of the type-II band alignment, photoexcited electron−hole pairs split in such a way that electrons accumulate in the CdSe core while holes do so in the peripherical CdTe crown.[3−6] The strong dielectric confinement of colloidal NPLs, set by the low polarizability of the capping ligands, provides sizable electron−hole attractions across the interface, hence preserving excitonic interactions.[4,7,8] With appropriate engineering, these structures are of interest for light harvesting, sub-band gap emission, infrared detection, fluorescence up-conversion, and low-threshold lasing.[1,2,9−12]

To date, the majority of studies on CdSe/CdTe NPLs have focused on the spectral and dynamic properties of neutral excitons (X^0).[3−6,8,10,11,13,14] However, electron−hole separation in type-II nanocrystals is known to suppress Auger processes,[15−17] which may prompt the formation of long-lived trions and biexciton species in photoexcited NPLs.[18] In addition, progress in the electrochemical charging of heteronanocrystals has recently reached deterministic and stable control of the number of confined carriers in individual particles.[19] This technique produces multiply charged excitons, where a few excess carriers interact with the photoexcited electron−hole pair while largely preserving the intrinsic behavior of the semiconductor. Charge control through doping is also advancing in this direction.[20−22] In this context, investigating the effect of discrete charging on the electronic structure and the ensuing optical properties of CdSe/CdTe NPLs is in order.

Early experimental studies in type-II quantum dot core/shell nanocrystals reported significant blue-shifts (20−200 meV) of the photoluminescence peak when switching from single excitons to multiexcitons or charged excitons.[15,23−25] Similar findings have been reported in other type-II and quasi-type-II heterostructures, such as nanorods,[1] tetrapods,[26] dot-in-rods,[27] and rod-in-rods.[28] The origin of these shifts is connected with the Coulomb interactions between the recombining exciton and the spectator charges. The latter introduce Coulomb repulsions, which—owing to the spatial separation of electrons and holes—are not compensated by attractions. Because the initial state of the optical transition has more carriers (and hence more repulsions) than the final one, the transition energy increases.[15,29,30]

The question arises of whether type-II core/crown NPLs behave similarly. The answer is not straightforward because NPLs have characteristic attributes that must be considered.

Received: February 3, 2022
Revised: April 4, 2022
Published: April 19, 2022

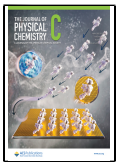

https://doi.org/10.1021/acs.jpcc.2c00827
J. Phys. Chem. C 2022, 126, 7152−7157

Unlike in quantum dots, the anisotropic shape and large (but finite) in-plane dimensions of NPLs place them in an intermediate confinement regime.[31,32] Carriers of the same sign may then separate over large distances to minimize repulsions. Also, attractive interactions across the CdSe/CdTe interface are stimulated by dielectric confinement.[4,7,8] It is then unclear if Coulomb repulsions will still prevail. In this work, we address these questions by means of computational simulations.

We use the same effective mass Hamiltonians which successfully described the emission features of neutral excitons in single CdSe/CdTe NPLs,[8] but now extended to the case of charged excitons (X^n, where n is the number of excess carriers, with n ranging from two extra holes, $n = 2$, to three extra electrons, $n = -3$) and that of biexcitons (XX). A full configuration interaction (CI) method is used to account for few-body interactions including correlation effects. We find that, as a result of the interplay between spatial and dielectric confinements, the emission spectra of typical CdSe/CdTe NPLs display a marked dependence on the number of spectator charges in terms of energy, oscillator strength, and bandwidth. Some of the effects we predict are as follows: (i) blue- and red-shifts of the band edge transition in an energy range over 100 meV around that of the neutral excitons, well beyond the typical shifts obtained by varying lateral confinement; (ii) the formation of multiple peaks at low temperature, which define the electronically limited bandwidth of these systems and can be exploited for multicolor emission; and (iii) the enhanced leakage of electrons outside the core when repulsions exceed the conduction band offset, which translates into a boost of the interband recombination rate and may be useful, for example, in the design of optical charge sensors.

METHODS

Calculations are carried within the k·p theory framework. Noninteracting (single-particle) electron and hole states are calculated with single-band Hamiltonians including the core/crown lattice mismatch strain in a continuum elastic model[8] and self-energy corrections to account for the dielectric mismatch.[33] The low temperature band gaps of CdSe (1.76 eV) and CdTe (1.6 eV) are taken from ref 34 and the rest of the material parameters from ref 35.

Many-body eigenstates and eigenenergies are calculated within the full CI method, using CI tool codes.[36] The Coulomb integrals for the CI matrix elements, including the enhancement coming from dielectric confinement, are calculated by solving the Poisson equation using Comsol 4.2. The CI basis set for CdSe/CdS NPLs is formed by all the possible combinations of the first 20 independent electron and 24 independent hole spin orbitals. Charged exciton and biexciton configurations are then defined by all the possible Hartree products between the few-electron and few-hole Slater determinants, consistent with spin and symmetry requirements. Optical spectra are calculated within the dipole approximation,[37] assuming Lorentzian bands with a linewidth of 1 meV.

RESULTS

We consider core/crown NPLs with typical dimensions.[3] The thickness is 4.5 atomic monolayers.

A crown with fixed lateral dimensions 20 × 30 nm^2 is taken, and the core size is 10 × 20 nm^2. Figure 1a shows the calculated emission spectrum at a temperature $T = 20$ K for different excitonic complexes. X^0 stands for a neutral exciton (one interacting electron−hole pair).

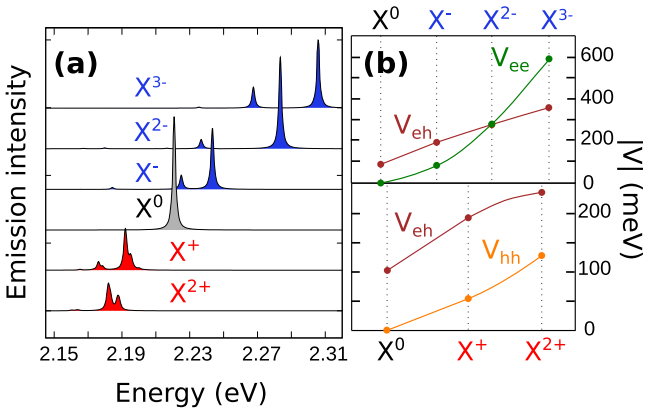

Figure 1. (a) Emission spectrum of neutral and charged excitons in a CdSe/CdTe NPL. (b) Corresponding mean value of Coulomb attractions and repulsions. Coulomb terms are depicted in absolute value. The spectra are simulated at 20 K. The core area is 10 × 20 nm^2.

When extra charges are introduced into the system, $X^{n\pm}$ complexes are formed, where n is the number of charges (positive or negative) added to the neutral exciton. As can be seen in the figure, varying the number of charges in the NPL has a substantial effect on the optical spectrum. Negatively charged excitons become increasingly blue-shifted, while positively charged excitons are red-shifted instead. In both cases, charging leads to multipeaked emissions.

The energetic shift between X^{2+} and X^{3-}, over 100 meV, is of considerable magnitude. It is larger than the spectral shifts one can obtain in colloidal NPLs by modifying the weak lateral confinement (a few tens of meV).[38,39] It is also much larger than the typical shifts observed upon charging type-I NPLs.[40−42] The origin is connected with the unbalanced repulsive and attractive Coulomb interactions in the type-II NPL. To gain a semiquantitative understanding, we compare the relative strengths of attractions and repulsions for each excitonic complex. We calculate the expectation value of the terms contributing to the total energy of $X^{n\pm}$

$$\langle E_{tot}\rangle = \langle E_e\rangle + \langle E_h\rangle + \langle V_{eh}\rangle + \langle V_{ee}\rangle + \langle V_{hh}\rangle \quad (1)$$

here, E_{tot} is the total energy of the $X^{n\pm}$ ground state, E_e (E_h) is the sum of the energies of the noninteracting electrons (holes) forming the complex, V_{eh} is the sum of the attractions between electron−hole pairs, and V_{ee} (V_{hh}) is that of the electron−electron (hole−hole) repulsions. Figure 1b compares the absolute values of repulsions and attractions for X^{n-} (top panel) and X^{n+} (bottom panel). In both cases, the attractions $<V_{eh}>$ increase (in absolute value) with the number of carriers because the electron finds more holes to interact with (or vice versa) across the CdSe/CdTe interface. The repulsions show, however, contrasting behaviors for electrons and holes. $<V_{ee}>$ shows a rapid − superlinear − increase, reflecting the strong electron−electron interactions within the CdSe core, and leads to repulsions surpassing attractions in X^{n-}. By contrast, holes are localized in the CdTe crown, with a large core separating the two symmetric sides. This yields relatively weak repulsions, $<V_{hh}>$, which remain smaller than attractions. In short, in X^{n-}

https://doi.org/10.1021/acs.jpcc.2c00827
J. Phys. Chem. C 2022, 126, 7152−7157

repulsions prevail over attractions, while in X^{n+} the opposite holds. This is directly connected to the blue-shift (red-shift) observed in Figure 1a. It follows from Figure 1 that, in spite of the weak lateral confinement, Coulomb interactions permit using the number of extra charges injected in type-II NPLs as a tool for broad and reversible tuning of the emission wavelengths around the value set by the NPL thickness. The same finding holds at room temperature, see Figure S1. It is worth noting that the blue-shift of the excitonic peak in the presence of excess electrons is partly reminiscent of the dynamical screening reported in highly doped semiconductors,[43] albeit in the few-particle limit.

As for the multipeaked emission of charged species in Figure 1a, it arises from transitions involving not only the band edge states but also high-spin states at low energy,[8] with small satellites further arising from shake-up processes.[44,45] These peaks set the electronic limit of the bandwidth (which is greater for charged excitons than for X^0) and might be of interest for multi-color emission.[46] A detailed spectral assignment of the trion states (X^- and X^+) is provided in the Supporting Information, Figures S2 and S3.

We next move to the study of biexcitons. In Figure 2a we compare X^0 and XX emission spectra for NPLs with variable core dimensions. The core width is fixed at 10 nm, but the length L_y^c is varied. By increasing L_y^c, the shift between X^0 and XX peaks evolves from strongly antibonding (~40 meV blue-shift, L_y^c = 20 nm) to nearly nonbonding character (~5 meV, L_y^c = 20 nm). The tunability of the spectral shift holds at room temperature as well, see Figure S4. This magnitude is similar to that reported for type-II core/shell nanocrystals,[29] but here it is achieved within the weak confinement regime, which permits keeping associated physical phenomena, such as reduced Auger relaxation[47] and giant oscillator strength effects.[7,48]

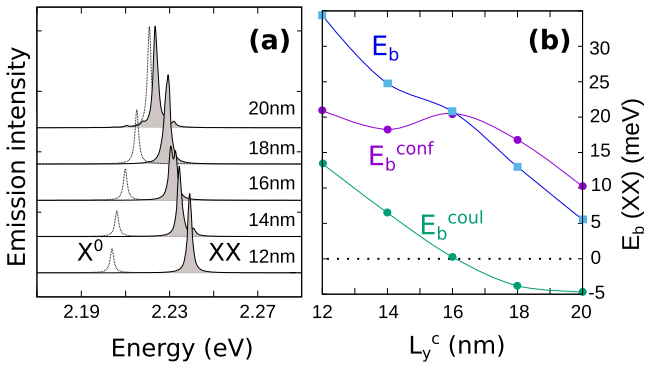

Figure 2. (a) Comparison between the emission spectrum of biexcitons and excitons for different core lengths, L_y^c. (b) Corresponding biexciton binding energy, along with its kinetic and Coulomb contributions (see text). The spectra are simulated at 20 K. The core width is 10 nm.

The physical origin of the shift is different from that of nanocrystals, as we will explain next. In both cases, the emission peak is mainly related to the band edge transition (see Figure S5 for a detailed spectral assignment of the XX emission band). Thus, the spectral shift between XX and X^0 corresponds to the biexciton binding energy, $E_b(XX) = E_{tot}(XX) - 2E_{tot}(X)$ (here, $E_b(XX)>0$ means unbound biexciton). Using expectation values, eq 1, $E_b(XX)$ can be decomposed as

$$\langle E_b(XX)\rangle = \langle E^{coul}\rangle + \langle E^{conf}\rangle \quad (2)$$

here,

$$E^{coul} = V_{eh}(XX) + V_{ee}(XX) + V_{hh}(XX) - 2V_{eh}(X^0) \quad (3)$$

is the contribution is associated with changes in the relative strength of Coulomb interactions. In turn,

$$E^{conf} = (E_e(XX) - 2E_e(X^0)) + (E_h(XX) - 2E_h(X^0)) \quad (4)$$

is the spatial confinement contribution to the binding energy, associated with changes in the energy of occupied single-particle spin orbitals. In strongly confined quantum dots and nanocrystals, the energy spacing between consecutive orbitals exceeds Coulomb repulsions. Then, both XX and X^0 have electrons (holes) in the $1S_e$ ($1S_h$) orbital, which gives $E^{conf} \approx 0$. The biexciton shift is thus well explained by changes in E^{coul} alone.[29,49] However, NPLs are in a strongly correlated regime. Coulomb repulsions (of the order of ~100 meV, see Figure 1b) exceed the spacing between consecutive orbitals (~10 meV[8]). This promotes the occupation of excited orbitals to minimize repulsions, making E^{conf} significant. As a matter of fact, Figure 2b shows that E^{conf} is the dominant term in $E_b(XX)$. With increasing L_y^c values, repulsions in the core

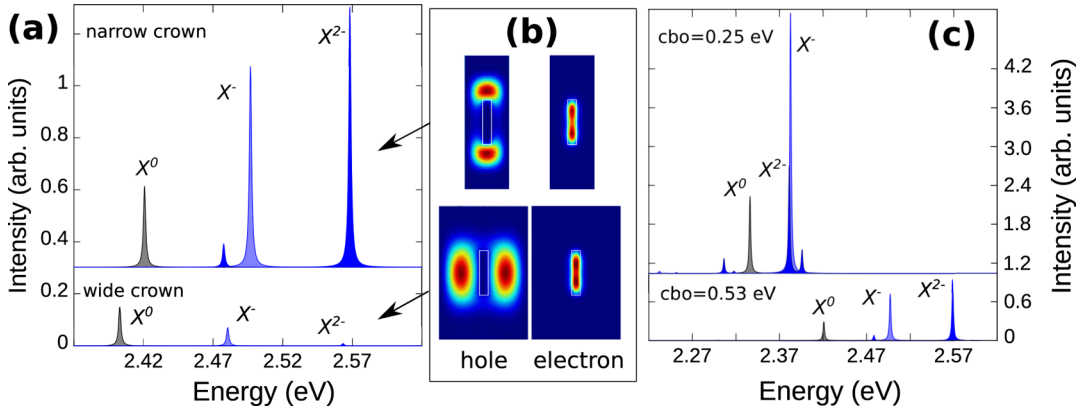

Figure 3. (a) Emission spectrum of X^0, X^-, and X^{2-} for NPLs with wide (20 × 30 nm^2) and narrow (10 × 30 nm^2) crowns. (b) Corresponding the hole (left) and two-electron (right) charge densities for X^-. (c) Emission spectrum of the narrow crown NPL, now comparing the conduction band offset of 0.53 eV (as in CdSe/CdTe) with 0.25 eV (as in CdSe/$CdSe_{0.5}Te_{0.5}$). The spectra are simulated at 4 K and are offset vertically for clarity.

https://doi.org/10.1021/acs.jpcc.2c00827
J. Phys. Chem. C 2022, 126, 7152−7157

decrease, and so does E^{coul}. However, at $L_y^c = 16$ nm, when $E^{coul} \approx 0$ (attractions equal repulsions), the biexciton is unbound, $E_b(XX) \approx 20$ meV. This is because confinement terms, E^{conf}, are still important.

We have so far shown the potential of Coulomb repulsions to modulate the emission energy of charged excitons and biexcitons in type-II NPLs. The last question we address is whether a similar modulation can be achieved on the emission rate. In type-I NPLs, trions ($X^{\pm}$) have smaller oscillator strength than excitons (X^0)[40] because the giant oscillator strength effect is diluted.[42] In Figure 1a, however, no major change is observed between X^0 and $X^{n\pm}$, which suggests that in type-II NPLs, the reduced electron−hole overlap gives rise to a distinct behavior. In what follows, we show that substantial modulation of the oscillator strength can be obtained if one uses a proper structural design in which Coulomb interactions are exploited to force a transition from the type-II to quasi-type-II localization of charged excitons. To illustrate this effect, we consider two NPLs with the same core (2×10 nm^2) but different crown dimensions: 20×30 nm^2 versus 10×30 nm^2. Figure 3a compares the resulting emission spectrum for X^0, X^-, and X^{2-} in both NPLs. Clearly, the narrow-crown NPL shows a gradual enhancement of the intensity as the number of electrons increases, which is not observed in the wide-crown NPL. The different responses are related to the localization of holes in each crown. As shown in Figure 3b, in a wide crown, the hole charge density exhibits transversal localization, while in a narrow crown, lateral confinement favors longitudinal localization. In turn, the electron charge density is similar in both geometries. When the number of electrons increases, Coulomb repulsions stretch the electron density along the longitudinal axis of the core (see e.g., electron charge density of X^- in Figure 3b, which shows the electrons are off-centered). This enhances leakage into the crown, which results in stronger electron−hole overlap − and hence greater emission intensity − in the narrow-crown configuration only.

Further enhancement of the intensity can be obtained by reducing the conduction band offset, for example, by using alloyed (CdSeTe) crowns.[46,50] To estimate the magnitude of this effect, in Figure 3c we compare the emission of the narrow CdSe/CdTe NPL to that of the same NPL with a halved conduction band offset (close to that of $CdSe_{0.5}Te_{0.5}$). One can see that in the latter case, a greater increase in the emission intensity is obtained when the number of electrons increases (cf. X^0 and X^-). This is because electron−electron repulsions find it easier to overcome the crown potential barrier and increase the leakage outside the core.

All in all, Figure 3 shows that the emission intensity of CdSe/CdTe NPLs can be modulated through the number of injected electrons in the core. With appropriate structural design, Coulomb interactions make excitonic species gradually reduce their indirect character. Electron−electron repulsions play an important role in this regard by prompting electron delocalization outside the core, but it is worth noting that so do electron−hole attractions (see Figure S6). This carrier-sensitive optical response could be interesting for ratiometric probing of charges in the NPL.

CONCLUSIONS

In conclusion, we have shown that the number of carriers confined in type-II colloidal NPLs is a versatile tool to control the electronic structure. Coulomb repulsions can prevail over attractions in spite of the weak lateral confinement in these systems. As a result, we predict that the emission spectra of typical CdSe/CdTe NPLs will display a marked dependence on the number of spectator charges in terms of energy, oscillator strength, and homogeneous bandwidth. The emission peak is red-shifted when charging with extra holes, but blue-shifted instead when charging with electrons or another exciton. The dimensions of the core and the crown can be used to tailor the magnitude of these effects efficiently. This behavior extends the photophysics of type-II quantum dot nanocrystals to NPLs while preserving the advantages of quasi-two-dimensional systems.

ASSOCIATED CONTENT

Supporting Information

The Supporting Information is available free of charge at https://pubs.acs.org/doi/10.1021/acs.jpcc.2c00827.

Additional calculations on emission spectra at high temperature, spectral assignments for trions and biexcitons, and effect of electron−hole attraction on the emission of CdSe/CdTe NPLs are given (PDF)

AUTHOR INFORMATION

Corresponding Author

Juan I. Climente − *Departament de Química Física i Analítica, Universitat Jaume I, Castelló de la Plana E-12080, Spain*; orcid.org/0000-0001-6984-6424; Email: climente@uji.es

Author

Jordi Llusar − *Departament de Química Física i Analítica, Universitat Jaume I, Castelló de la Plana E-12080, Spain*

Complete contact information is available at: https://pubs.acs.org/10.1021/acs.jpcc.2c00827

Notes

The authors declare no competing financial interest.

ACKNOWLEDGMENTS

The authors acknowledge support from the MICINN CTQ2017-83781-P and UJI-B2021-06 projects. We are grateful to Iwan Moreels, Thierry Barisien, and Josep Planelles for discussions.

REFERENCES

(1) Lo, S. S.; Mirkovic, T.; Chuang, C.-H.; Burda, C.; Scholes, G. D. Emergent Properties Resulting From Type-II Band Alignment in Semiconductor Nanoheterostructures. *Adv. Mater.* **2011**, *23*, 180−197.

(2) Dorfs, D.; Franzl, T.; Osovsky, R.; Brumer, M.; Lifshitz, E.; Klar, T. A.; Eychmüller, A. Type-I and Type-II Nanoscale Heterostructures Based on CdTe Nanocrystals: A Comparative Study. *Small* **2008**, *4*, 1148−1152.

(3) Pedetti, S.; Ithurria, S.; Heuclin, H.; Patriarche, G.; Dubertret, B. Type-II CdSe/CdTe Core/Crown Semiconductor Nanoplatelets. *J. Am. Chem. Soc.* **2014**, *136*, 16430−16438.

(4) Antanovich, A. V.; Prudnikau, A. V.; Melnikau, D.; Rakovich, Y. P.; Chuvilin, A.; Woggon, U.; Achtstein, A. W.; Artemyev, M. V. Colloidal Synthesis and Optical Properties of Type-II CdSe−CdTe and Inverted CdTe−CdSe Core−Wing Heteronanoplatelets. *Nanoscale* **2015**, *7*, 8084−8092.

(5) Kelestemur, Y.; Olutas, M.; Delikanli, S.; Guzelturk, B.; Akgul, M. Z.; Demir, H. V. Type-II Colloidal Quantum Wells: CdSe/CdTe Core/Crown Heteronanoplatelets. *J. Phys. Chem. C* **2015**, *119*, 2177−2185.

(6) Wu, K.; Li, Q.; Jia, Y.; McBride, J. R.; Xie, Z.-X.; Lian, T. Efficient and Ultrafast Formation of Long-Lived Charge-Transfer Exciton State in Atomically Thin Cadmium Selenide/Cadmium Telluride Type-II Heteronanosheets. *ACS Nano* **2015**, *9*, 961−968.
(7) Scott, R.; Kickhöfel, S.; Schoeps, O.; Antanovich, A.; Prudnikau, A.; Chuvilin, A.; Woggon, U.; Artemyev, M.; Achtstein, A. W. Temperature Dependent Radiative and Non-radiative Recombination Dynamics in CdSe−CdTe and CdTe−CdSe Type II Hetero Nanoplatelets. *Phys. Chem. Chem. Phys.* **2016**, *18*, 3197−3203.
(8) Steinmetz, V.; Climente, J. I.; Pandya, R.; Planelles, J.; Margaillan, F.; Puttisong, Y.; Dufour, M.; Ithurria, S.; Sharma, A.; Lakhwani, G.; et al. Emission State Structure and Linewidth Broadening Mechanisms in Type-II CdSe/CdTe Core-Crown Nanoplatelets: A Combined Theoretical - Single Nanocrystal Optical Study. *J. Phys. Chem. C* **2020**, *124*, 17352−17363.
(9) Min, Y.; Im, E.; Hwang, G.-T.; Kim, J.-W.; Ahn, C.-W.; Choi, J.-J.; Hahn, B.-D.; Choi, J.-H.; Yoon, W.-H.; Park, D.-S.; et al. Heterostructures in Two-Dimensional Colloidal Metal Chalcogenides: Synthetic Fundamentals and Applications. *Nano Res.* **2019**, *12*, 1750−1769.
(10) Li, Q.; Zhou, B.; McBride, J. R.; Lian, T. Efficient Diffusive Transport of Hot and Cold Excitons in Colloidal Type II CdSe/CdTe Core/Crown Nanoplatelet Heterostructures. *ACS Energy Lett.* **2017**, *2*, 174−181.
(11) Khan, A. H.; Bertrand, G. H. V.; Teitelboim, A.; Sekhar, M. C.; Polovitsyn, A.; Brescia, R.; Planelles, J.; Climente, J. I.; Oron, D.; Moreels, I. CdSe/CdS/CdTe Core/Barrier/Crown Nanoplatelets: Synthesis, Optoelectronic Properties, and Multiphoton Fluorescence Upconversion. *ACS Nano* **2020**, *14*, 4206−4215.
(12) Li, Q.; Xu, Z.; McBride, J. R.; Lian, T. Low Threshold Multiexciton Optical Gain in Colloidal CdSe/CdTe Core/Crown Type-II Nanoplatelet Heterostructures. *ACS Nano* **2017**, *11*, 2545−2553.
(13) Pandya, R.; Chen, R. Y. S.; Cheminal, A.; Dufour, M.; Richter, J. M.; Thomas, T. H.; Ahmed, S.; Sadhanala, A.; Booker, E. P.; Divitini, G.; et al. Exciton−Phonon Interactions Govern Charge-Transfer-State Dynamics in CdSe/CdTe Two-Dimensional Colloidal Heterostructures. *J. Am. Chem. Soc.* **2018**, *140*, 14097−14111.
(14) Pandya, R.; Steinmetz, V.; Puttisong, Y.; Dufour, M.; Chen, W. M.; Chen, R. Y. S.; Barisien, T.; Sharma, A.; Lakhwani, G.; Mitioglu, A.; et al. Fine Structure and Spin Dynamics of Linearly Polarized Indirect Excitons in Two-Dimensional CdSe/CdTe Colloidal Heterostructures. *ACS Nano* **2019**, *13*, 10140−10153.
(15) Oron, D.; Kazes, M.; Banin, U. Multiexcitons in Type-II Colloidal Semiconductor Quantum Dots. *Phys. Rev. B: Condens. Matter Mater. Phys.* **2007**, *75*, 035330.
(16) Climente, J. I.; Movilla, J. L.; Planelles, J. Auger Recombination Suppression in Nanocrystals With Asymmetric Electron−Hole Confinement. *Small* **2012**, *8*, 754−759.
(17) Philbin, J. P.; Rabani, E. Auger Recombination Lifetime Scaling for Type I and Quasi-Type II Core/Shell Quantum Dots. *J. Phys. Chem. Lett.* **2020**, *11*, 5132−5138.
(18) Wang, J.-H.; Liang, G.-J.; Wu, K.-F. Long-Lived Single Excitons, Trions, and Biexcitons in CdSe/CdTe Type-II Colloidal Quantum Wells. *Chin. J. Chem. Phys.* **2017**, *30*, 649−656.
(19) Morozov, S.; Pensa, E. L.; Khan, A. H.; Polovitsyn, A.; Cortés, E.; Maier, S. A.; Vezzoli, S.; Moreels, I.; Sapienza, R. Electrical Control of Single-Photon Emission in Highly Charged Individual Colloidal Quantum Dots. *Sci. Adv.* **2020**, *6*, No. eabb1821.
(20) Capitani, C.; Pinchetti, V.; Gariano, G.; Santiago-González, B.; Santambrogio, C.; Campione, M.; Prato, M.; Brescia, R.; Camellini, A.; Bellato, F.; et al. Quantized Electronic Doping towards Atomically Controlled "Charge-Engineered" Semiconductor Nanocrystals. *Nano Lett.* **2019**, *19*, 1307−1317.
(21) Dutta, A.; Medda, A.; Patra, A. Recent Advances and Perspectives on Colloidal Semiconductor Nanoplatelets for Optoelectronic Applications. *J. Phys. Chem. C* **2020**, *125*, 20−30.
(22) Diroll, B. T.; Cho, W.; Coropceanu, I.; Harvey, S. M.; Brumberg, A.; Holtgrewe, N.; Crooker, S. A.; Wasielewski, M. R.; Prakapenka, V. B.; Talapin, D. V.; et al. Semiconductor Nanoplatelet Excimers. *Nano Lett.* **2018**, *18*, 6948−6953.
(23) Bang, J.; Chon, B.; Won, N.; Nam, J.; Joo, T.; Kim, S. Spectral Switching of Type-II Quantum Dots by Charging. *J. Phys. Chem. C* **2009**, *113*, 6320−6323.
(24) Qin, W.; Guyot-Sionnest, P. Evidence for the Role of Holes in Blinking: Negative and Oxidized CdSe/CdS Dots. *ACS Nano* **2012**, *6*, 9125−9132.
(25) Ivanov, S. A.; Achermann, M. Spectral and Dynamic Properties of Excitons and Biexcitons in Type-II Semiconductor Nanocrystals. *ACS Nano* **2010**, *4*, 5994−6000.
(26) Golinskaya, A. D.; Smirnov, A. M.; Kozlova, M. V.; Zharkova, E. V.; Vasiliev, R. B.; Mantsevich, V. N.; Dneprovskii, V. S. Tunable blue-shift of the charge-transfer photoluminescence in tetrapod-shaped CdTe/CdSe nanocrystals. *Results Phys.* **2021**, *27*, 104488.
(27) Saba, M.; Minniberger, S.; Quochi, F.; Roither, J.; Marceddu, M.; Gocalinska, A.; Kovalenko, M. V.; Talapin, D. V.; Heiss, W.; Mura, A.; et al. Exciton−Exciton Interaction and Optical Gain in Colloidal CdSe/CdS Dot/Rod Nanocrystals. *Adv. Mater.* **2009**, *21*, 4942−4946.
(28) Christodoulou, S.; Rajadell, F.; Casu, A.; Vaccaro, G.; Grim, J. Q.; Genovese, A.; Manna, L.; Climente, J. I.; Meinardi, F.; Rainò, G.; et al. Band Structure Engineering via Piezoelectric Fields in Strained Anisotropic CdSe/CdS Nanocrystals. *Nat. Commun.* **2015**, *6*, 1−8.
(29) Piryatinski, A.; Ivanov, S. A.; Tretiak, S.; Klimov, V. I. Effect of Quantum and Dielectric Confinement on the Exciton−Exciton Interaction Energy in Type II Core/Shell Semiconductor Nanocrystals. *Nano Lett.* **2007**, *7*, 108−115.
(30) Tyrrell, E. J.; Smith, J. M. Effective Mass Modeling of Excitons in Type-II Quantum Dot Heterostructures. *Phys. Rev. B: Condens. Matter Mater. Phys.* **2011**, *84*, 165328.
(31) Rajadell, F.; Climente, J. I.; Planelles, J. Excitons in Core-Only, Core-Shell and Core-Crown CdSe Nanoplatelets: Interplay Between In-Plane Electron-Hole Correlation, Spatial Confinement, and Dielectric Confinement. *Phys. Rev. B* **2017**, *96*, 035307.
(32) Richter, M. Nanoplatelets as Material System Between Strong Confinement and Weak Confinement. *Phys. Rev. Mater.* **2017**, *1*, 016001.
(33) Movilla, J. L.; Planelles, J.; Climente, J. I. Dielectric Confinement Enables Molecular Coupling in Stacked Colloidal Nanoplatelets. *J. Phys. Chem. Lett.* **2020**, *11*, 3294−3300.
(34) Adachi, S. *Handbook on Physical Properties of Semiconductors*; Kluwer Academics, 2004; Vol. *3*.
(35) Llusar, J.; Planelles, J.; Climente, J. I. Strain in Lattice-Mismatched CdSe-Based Core/Shell Nanoplatelets. *J. Phys. Chem. C* **2019**, *123*, 21299−21306.
(36) Bertoni, A. CItool, 2011. https://github.com/andreabertoni/citool (accessed May 4, 2021).
(37) Jacak, L.; Hawrylak, P.; Wojs, A. *Quantum Dots*; Springer, 1998.
(38) Bertrand, G. H. V.; Polovitsyn, A.; Christodoulou, S.; Khan, A. H.; Moreels, I. Shape Control of Zincblende CdSe Nanoplatelets. *Chem. Commun.* **2016**, *52*, 11975−11978.
(39) Di Giacomo, A.; Rodà, C.; Khan, A. H.; Moreels, I. Colloidal Synthesis of Laterally Confined Blue-Emitting 3.5 Monolayer CdSe Nanoplatelets. *Chem. Mater.* **2020**, *32*, 9260−9267.
(40) Ayari, S.; Quick, M. T.; Owschimikow, N.; Christodoulou, S.; Bertrand, G. H. V.; Artemyev, M.; Moreels, I.; Woggon, U.; Jaziri, S.; Achtstein, A. W. Tuning Trion Binding Energy and Oscillator Strength in a Laterally Finite 2D System: CdSe Nanoplatelets as a Model System for Trion Properties. *Nanoscale* **2020**, *12*, 14448−14458.
(41) Peng, L.; Otten, M.; Hazarika, A.; Coropceanu, I.; Cygorek, M.; Wiederrecht, G. P.; Hawrylak, P.; Talapin, D. V.; Ma, X. Bright Trion Emission From Semiconductor Nanoplatelets. *Phys. Rev. Mater.* **2020**, *4*, 056006.
(42) Macias-Pinilla, D. F.; Planelles, J.; Mora-Seró, I.; Climente, J. I. Comparison Between Trion and Exciton Electronic Properties in CdSe and PbS Nanoplatelets. *J. Phys. Chem. C* **2021**, *125*, 15614−15622.

https://doi.org/10.1021/acs.jpcc.2c00827
J. Phys. Chem. C 2022, 126, 7152−7157

(43) Gao, S.; Liang, Y.; Spataru, C. D.; Yang, L. Dynamical Excitonic Effects in Doped Two-Dimensional Semiconductors. *Nano Lett.* **2016**, *16*, 5568−5573.
(44) Antolinez, F. V.; Rabouw, F. T.; Rossinelli, A. A.; Cui, J.; Norris, D. J. Observation of Electron Shakeup in CdSe/CdS Core/Shell Nanoplatelets. *Nano Lett.* **2019**, *19*, 8495−8502.
(45) Llusar, J.; Climente, J. I. Nature and Control of Shakeup Processes in Colloidal Nanoplatelets. *ACS Photonics* **2020**, *7*, 3086−3095.
(46) Dufour, M.; Steinmetz, V.; Izquierdo, E.; Pons, T.; Lequeux, N.; Lhuillier, E.; Legrand, L.; Chamarro, M.; Barisien, T.; Ithurria, S. Engineering Bicolor Emission in 2D Core/Crown CdSe/$CdSe_{1-x}$ Te_x Nanoplatelet Heterostructures Using Band-Offset Tuning. *J. Phys. Chem. C* **2017**, *121*, 24816−24823.
(47) Kunneman, L. T.; Tessier, M. D.; Heuclin, H.; Dubertret, B.; Aulin, Y. V.; Grozema, F. C.; Schins, J. M.; Siebbeles, L. D. A. Bimolecular Auger Recombination of Electron−Hole Pairs in Two-Dimensional Cdse and CdSe/CdZnS Core/Shell Nanoplatelets. *J. Phys. Chem. Lett.* **2013**, *4*, 3574−3578.
(48) Planelles, J.; Achtstein, A. W.; Scott, R.; Owschimikow, N.; Woggon, U.; Climente, J. I. Tuning Intraband and Interband Transition Rates via Excitonic Correlation in Low-Dimensional Semiconductors. *ACS Photonics* **2018**, *5*, 3680−3688.
(49) Dalgarno, P. A.; Smith, J. M.; McFarlane, J.; Gerardot, B. D.; Karrai, K.; Badolato, A.; Petroff, P. M.; Warburton, R. J. Coulomb Interactions in Single Charged Self-Assembled Quantum Dots: Radiative Lifetime and Recombination Energy. *Phys. Rev. B: Condens. Matter Mater. Phys.* **2008**, *77*, 245311.
(50) Kelestemur, Y.; Guzelturk, B.; Erdem, O.; Olutas, M.; Erdem, T.; Usanmaz, C. F.; Gungor, K.; Demir, H. V. CdSe/$CdSe_{1-x}$ Te_x Core/Crown Heteronanoplatelets: Tuning the Excitonic Properties without Changing the Thickness. *J. Phys. Chem. C* **2017**, *121*, 4650−4658.

https://doi.org/10.1021/acs.jpcc.2c00827
J. Phys. Chem. C 2022, 126, 7152−7157